Impact of anisotropic atomic motions in proteins on powder-averaged incoherent neutron scattering intensities

Gerald R. Kneller and Guillaume Chevrot

Citation: J. Chem. Phys. **137**, 225101 (2012); doi: 10.1063/1.4769782
View online: http://dx.doi.org/10.1063/1.4769782
View Table of Contents: http://jcp.aip.org/resource/1/JCPSA6/v137/i22
Published by the American Institute of Physics.

Impact of anisotropic atomic motions in proteins on powder-averaged incoherent neutron scattering intensities

Gerald R. Kneller[1,2,3,a] and Guillaume Chevrot[1,2]
[1]*Centre de Biophys. Moléculaire, CNRS; Rue Charles Sadron, 45071 Orléans, France*
[2]*Synchrotron Soleil, L'Orme de Merisiers, 91192 Gif-sur-Yvette, France*
[3]*Université d'Orléans, Chateau de la Source-Av. du Parc Floral, 45067 Orléans, France*

(Received 23 September 2012; accepted 19 November 2012; published online 11 December 2012)

This paper addresses the question to which extent anisotropic atomic motions in proteins impact angular-averaged incoherent neutron scattering intensities, which are typically recorded for powder samples. For this purpose, the relevant correlation functions are represented as multipole series in which each term corresponds to a different degree of intrinsic motional anisotropy. The approach is illustrated by a simple analytical model and by a simulation-based example for lysozyme, considering in both cases the elastic incoherent structure factor. The second example shows that the motional anisotropy of the protein atoms is considerable and contributes significantly to the scattering intensity. © *2012 American Institute of Physics*. [http://dx.doi.org/10.1063/1.4769782]

I. INTRODUCTION

Neutron scattering has proven to be a powerful tool for investigating the structure and dynamics of condensed matter on the atomic scale. Due to the dominant incoherent scattering cross section of hydrogen[1,2] it is essentially the sample-averaged single-particle dynamics of these atoms which is probed in neutron scattering experiments. References 3 and 4 give an overview on applications for studying, respectively, polymer and protein systems, in which hydrogen accounts for about 50% of the total number of atoms. A basic quantity which can be obtained from elastic incoherent neutron scattering is the mean square position fluctuation (MSPF) of the hydrogen atoms in the sample, $\mathrm{MSPF} = \langle u^2 \rangle$, where $u = \sqrt{(\mathbf{x} - \langle \mathbf{x} \rangle)^2}$ and $\mathbf{x}$ is the position of the scattering atom. It is, unfortunately, also customary to use the term "mean square displacement" (MSD) for $\langle u^2 \rangle$ (see, e.g., Ref. 4), which is a permanent source of confusion with the time-dependent MSD.[5] The latter is defined as $\mathrm{MSD}(t) = \langle (\mathbf{x}(t) - \mathbf{x}(0))^2 \rangle$, with "$t$" being the time lag with respect to an arbitrarily chosen time origin "0." For this reason, we use here the term "mean square position fluctuation." The MSPF is usually extracted from the elastic incoherent structure factor (EISF) and plays a central role in the study of the dynamical transition of proteins.[6–8] From its temperature dependence, one can, for example, derive a softness parameter which is related to protein function.[9] The usual method to extract MSPFs from experimental EISF data is based on the assumption that the EISF has the simple isotropic Gaussian form

$$\mathrm{EISF}(q) \approx \exp(-q^2 \langle u^2 \rangle / 3), \tag{1}$$

where $q = |\mathbf{q}|$ is the modulus of the momentum transfer vector in units of $\hbar$. The samples are supposed to be macroscopically isotropic, such that the observed EISF is the angular average of the $\mathbf{q}$-dependent EISF over the directions of $\mathbf{q}$,

$$\mathrm{EISF}(q) \equiv \overline{\mathrm{EISF}(\mathbf{q})}. \tag{2}$$

Most neutron scattering experiments on proteins are performed for hydrated protein powders and for this reason expression (2) is often referred to as "powder average." The approximation (1) is strictly valid only if all atoms in the system move in an isotropic harmonic potential of identical curvature. Motional heterogeneity, anharmonicity, and anisotropy of the local potential lead to a deviation of the EISF from the isotropic Gaussian form (1), which is in general only valid if $q^2 \langle u^2 \rangle \ll 1$. Computer simulations are a particularly useful tool to investigate the importance of non-Gaussian effects in the EISF by an "*ab initio*" approach and several studies with this aim have been undertaken in the past.[10–14] Concerning the particular aspect of anisotropic atomic motions, most simulation work in relation to experimental data concerns X-ray diffraction, since this technique gives site-specific information on atomic motion, including anisotropy.[15–17] To our knowledge, Ref. 11 is the only work in which the impact of anisotropic motions on neutron scattering intensities is explicitly discussed. The authors propose the quantity $S_{2,\mathrm{aniso}}(\mathbf{q}) = \exp(-\langle \mathbf{q} \cdot \mathbf{u} \rangle^2) - \exp(-q^2 \langle u^2 \rangle / 3)$ as an approximative measure for the motional anisotropy of a single atom (here the notation is slightly changed). They find that anisotropic atomic motions have a negligible impact on the total EISF and the result is explained by a mutual cancellation of the individual atomic contributions. It is, however, important to note that the validity of the proposed anisotropy measure is limited by the Gaussian approximation, $\mathrm{EISF}(\mathbf{q}) \approx \exp(-\langle \mathbf{q} \cdot \mathbf{u} \rangle^2)$, which implies that the scattering atom moves in a harmonic, possibly anisotropic potential. Moreover, depending explicitly on the direction of $\mathbf{q}$, it does not quantify the intrinsic anisotropy of the atomic motions in the system under consideration, which is probed by neutron scattering experiments from powder samples.

To look deeper into the question in how far motional anisotropy influences the form of powder-averaged incoherent neutron scattering intensities, we develop in this paper a general framework to quantify this effect. Our approach is based on appropriate multipole expansions of the relevant

[a]Electronic mail: gerald.kneller@cnrs-orleans.fr.

correlation functions and we discuss in particular the impact of motional anisotropy on the EISF and its cumulant expansion. The theoretical description of anisotropy effects is illustrated with an analytical example and with a molecular dynamics (MD) simulation study of lysozyme. The paper is organized as follows: Sec. II is devoted to the presentation of the theoretical part, Sec. III contains the presentation of the two examples, and the paper is concluded by a summary and a short discussion of the results.

II. THEORY

A. Neutron scattering

The basic quantity measured in neutron scattering is the dynamic structure factor,[1,2] $\mathcal{S}(\mathbf{q},\omega)$, which is the Fourier transform of the weighted double sum of quantum time correlation functions, $\mathcal{F}(\mathbf{q},t)$, involving the positions $\mathbf{x}_\alpha$ of the atomic nuclei in the scattering system,

$$\mathcal{S}(\mathbf{q},\omega) = \frac{1}{2\pi}\int_{-\infty}^{+\infty} dt\ \exp(-i\omega t)\mathcal{F}(\mathbf{q},t), \tag{3}$$

$$\mathcal{F}(\mathbf{q},t) = \sum_{\alpha,\beta}\{b^*_{\alpha,\mathrm{coh}}b_{\beta,\mathrm{coh}} + \delta_{\alpha,\beta}|b_{\alpha,\mathrm{inc}}|^2\} \times\langle\exp(i\mathbf{q}\cdot\mathbf{x}_\alpha(t))\exp(-i\mathbf{q}\cdot\mathbf{x}_\beta(0))\rangle. \tag{4}$$

Here, $\mathbf{q}$ and ω are, respectively, the momentum and energy transfer from the neutron to the sample in units of $\hbar$ and $\mathcal{F}(\mathbf{q},t)$ is called the total intermediate scattering function (ISF). The brackets $\langle\dots\rangle$ denote a quantum equilibrium ensemble average over the initial positions $\mathbf{x}_\alpha \equiv \mathbf{x}_\alpha(0)$ and the argument t is a lag time with respect to the time origin "0." Since the sample is supposed to be in thermal equilibrium, the arguments of $\mathbf{x}_\alpha$ and $\mathbf{x}_\beta$ in (4) can be shifted by an arbitrary value τ (stationarity). The quantities $b_{\alpha,\mathrm{coh}}$ and $b_{\alpha,\mathrm{inc}}$ are, respectively, the coherent and incoherent scattering length of atom α. They can be complex and determine the strength of the Fermi pseudopotential describing the neutron-nucleus interaction.[1,2] In contrast to X-ray diffraction and diffusion, there is no systematic relation between the scattering amplitude and the size of the scattering atom. As mentioned earlier, incoherent scattering from the smallest atom–hydrogen–dominates, in fact, all other scattering processes. In the following, we make the following assumptions:

1. The quantum time correlation functions appearing in the ISF can be replaced by their classical counterparts. This hypothesis is justified if the recoil energy of the scattering atom is much smaller than its thermal energy[18] and if quantum contributions to the ensemble averages can be neglected.
2. The scattering system contains a large number of hydrogen atoms, such that the contributions to the scattering intensity from the single-particle motions of these atoms dominate those from other atoms, as well as contributions from collective modes.
3. The motions of the scattering atoms are confined in space, such that the mean position of each atom is well defined.

If hypotheses 1 and 2 are verified, the ISF can be approximated by

$$\mathcal{F}(\mathbf{q},t) \approx N_\mathrm{H}|b_{\mathrm{H,inc}}|^2 F_{\mathrm{H,s}}(\mathbf{q},t), \tag{5}$$

where $F_{\mathrm{H,s}}(\mathbf{q},t)$ is the average self-scattering contribution from the N_H hydrogen atoms in the system,

$$F_{\mathrm{H,s}}(\mathbf{q},t) = \frac{1}{N_\mathrm{H}}\sum_{\alpha\in H}\langle\exp(i\mathbf{q}\cdot[\mathbf{x}_\alpha(t)-\mathbf{x}_\alpha(0)])\rangle. \tag{6}$$

The corresponding EISF is defined as the long-time limit

$$\mathrm{EISF_H}(\mathbf{q}) = \lim_{t\to\infty} F_{\mathrm{H,s}}(\mathbf{q},t). \tag{7}$$

For systems in thermodynamic equilibrium, one may write $\lim_{t\to\infty}\langle\exp(i\mathbf{q}\cdot[\mathbf{x}_\alpha(t)-\mathbf{x}_\alpha(0)])\rangle = |\langle\exp(i\mathbf{q}\cdot\mathbf{x}_\alpha)\rangle|^2$, which shows that the EISF is nonzero only if the mean values of the positions $\mathbf{x}_\alpha$ are bound, i.e., if the atomic motions are confined in space (assumption 3). In this case, the incoherent ISF probes effectively the displacements of the atomic positions with respect to their respective static averages,

$$\mathbf{u}_\alpha = \mathbf{x}_\alpha - \langle\mathbf{x}_\alpha\rangle, \tag{8}$$

and the EISF becomes

$$\mathrm{EISF_H}(\mathbf{q}) = \frac{1}{N_\mathrm{H}}\sum_{\alpha\in H}|\langle\exp(i\mathbf{q}\cdot\mathbf{u}_\alpha)\rangle|^2. \tag{9}$$

Assuming that the shifted correlation function $F'_{\mathrm{H,s}}(\mathbf{q},t) = F_{\mathrm{H,s}}(\mathbf{q},t) - \mathrm{EISF_H}(\mathbf{q})$ decays sufficiently quickly to zero, such that the corresponding Fourier transform exists, the dynamic structure factor can be cast into the form

$$S_{\mathrm{H,s}}(\mathbf{q},\omega) = \mathrm{EISF_H}(\mathbf{q})\delta(\omega) + \frac{1}{2\pi}\int_{-\infty}^{+\infty} dt\ \exp(-i\omega t)F'_{\mathrm{H,s}}(\mathbf{q},t), \tag{10}$$

which shows that EISF determines, in fact, the contribution from elastic scattering. In real experiments, one measures the convolution of expression (10) with the instrumental resolution.

B. Multipole expansion of the single-atom scattering functions

1. Intermediate scattering function

In the following, we consider incoherent neutron scattering from a single (hydrogen) atom and write the ISF in the compact form

$$F(\mathbf{q},t) = \langle\exp(i\mathbf{q}\cdot\mathbf{\Delta}(t))\rangle, \tag{11}$$

where $\mathbf{\Delta}(t)$ is the displacement of the scattering atom during the lag time t with respect to an arbitrarily chosen time origin,

$$\mathbf{\Delta}(t) = \mathbf{x}(t) - \mathbf{x}(0). \tag{12}$$

The dependencies of the ISF on the directions of both $\mathbf{q}$ and $\mathbf{\Delta}(t)$ can be separated by making use of the plane wave expansion[19]

$$\exp(i\mathbf{q}\cdot\mathbf{r}) = 4\pi\sum_{l=0}^{\infty}\sum_{m=-l}^{l} i^l j_l(qr)Y_{lm}(\Omega_q)Y^*_{lm}(\Omega_r), \tag{13}$$

where $q = |\mathbf{q}|$, $r = |\mathbf{r}|$, and Ω_q and Ω_r comprise, respectively, the spherical coordinates (θ, ϕ) of $\mathbf{q}$ and $\mathbf{r}$. The symbol $j_l(.)$ denotes the spherical Bessel function of first kind and order l and $Y_{lm}(.)$ are the spherical harmonics. Using identity (13), the ISF may be cast in the form of a multipole series,

$$F(\mathbf{q}, t) = 4\pi \sum_{l=0}^{\infty} \sum_{m=-l}^{l} i^l Y_{lm}(\Omega_q) \langle j_l(q\Delta(t)) Y^*_{lm}(\Omega_\Delta(t)) \rangle, \tag{14}$$

where $\Delta(t) = |\mathbf{\Delta}(t)|$ is the modulus of the displacement $\mathbf{\Delta}(t)$ and $\Omega_\Delta(t)$ defines its direction. As mentioned in the Introduction, incoherent neutron scattering experiments are usually performed on macroscopically isotropic samples. This corresponds to measuring the isotropic angular average

$$\overline{F(\mathbf{q}, t)} = \frac{1}{4\pi} \int d\Omega_q F(\mathbf{q}, t), \tag{15}$$

noting that $\int d\Omega_q \ldots = \int_0^\pi \int_0^{2\pi} \sin\theta d\theta d\phi \ldots$ is the integral over the directions of the momentum transfer vector expressed in spherical coordinates, $\mathbf{q} = (q \sin\theta \cos\phi, q \sin\theta \sin\phi, q \cos\theta)$. Inserting here the series (14), only the term for $l = 0$ is left on account of the orthonormality relation $\int d\Omega\, Y_{lm}(\Omega) Y^*_{l'm'}(\Omega) = \delta_{ll'}\delta_{mm'}$ of the spherical harmonics,

$$\overline{F(\mathbf{q}, t)} = \langle j_0(q\Delta(t)) \rangle. \tag{16}$$

A powder average removes thus all information about the motional anisotropy in the lag-time-dependent displacements $\mathbf{\Delta}(t)$.

In case of spatially confined motions, where $\mathbf{\Delta}(t) = \mathbf{u}(t) - \mathbf{u}(0)$, the ISF can be alternatively developed into a multipole series involving separately the directions of $\mathbf{u}(t)$ and $\mathbf{u}(0)$. Writing the ISF in the form $F(\mathbf{q}, t) = \langle \exp(i\mathbf{q} \cdot \mathbf{u}(t)) \exp(-i\mathbf{q} \cdot \mathbf{u}(0)) \rangle$ and applying the plane wave expansion to both factors in the ensemble average leads to

$$F(\mathbf{q}, t) = (4\pi)^2 \sum_{l=0}^{\infty} \sum_{l'=0}^{\infty} \sum_{m=-l}^{l} \sum_{m'=-l'}^{l'} Y^*_{l'm'}(\Omega_q) Y_{lm}(\Omega_q) \times \langle \varphi^*_{l'm'}(q, 0) \varphi_{lm}(q, t) \rangle, \tag{17}$$

where the variables $\varphi_{lm}(q, t)$ are defined as

$$\varphi_{lm}(q, t) = j_l(qu(t)) Y^*_{lm}(\Omega_u(t)). \tag{18}$$

The powder average leads here to the series

$$\overline{F(\mathbf{q}, t)} = \sum_{l=0}^{\infty} F_l(q, t), \tag{19}$$

where the coefficients $F_l(q, t)$ have the form

$$F_l(q, t) = 4\pi \sum_{m=-l}^{l} \langle \varphi^*_{lm}(q, 0) \varphi_{lm}(q, t) \rangle. \tag{20}$$

It follows from the transformation property of the spherical harmonics under rotations of the coordinate system[20,21] that the coefficients $F_l(q, t)$ are invariant under such transformations. Since they do not depend on the direction of $\mathbf{q}$, they can be considered as multipole coefficients containing information about the intrinsic anisotropy in the time-correlated displacements $\mathbf{u}$. If the latter are perfectly isotropic, the series (19) reduces to a single term

$$\overline{F(\mathbf{q}, t)} = \langle j_0(qu(t)) j_0(qu(0)) \rangle. \tag{21}$$

2. EISF

The multipole expansion of the EISF is obtained from expression (17) by performing the limit $t \to \infty$. Using that the time correlation function of any two variables a and b fulfills $\lim_{t\to\infty} \langle a(0)b(t) \rangle = \langle a \rangle \langle b \rangle$ if the system is in thermodynamic equilibrium, one obtains a series of the form

$$\begin{aligned} &\mathrm{EISF}(\mathbf{q}) \\ &= |\langle \exp(i\mathbf{q} \cdot \mathbf{u}) \rangle|^2 \\ &= (4\pi)^2 \sum_{l=0}^{\infty} \sum_{l'=0}^{\infty} \sum_{m=-l}^{l} \sum_{m'=-l'}^{l'} Y_{lm}(\Omega_q) Y^*_{l'm'}(\Omega_q) a_{lm}(q) a^*_{l'm'}(q), \end{aligned} \tag{22}$$

where the amplitudes $a_{lm}(q)$ are given by

$$a_{lm}(q) = \langle j_l(qu) Y^*_{lm}(\Omega_u) \rangle = \langle \varphi_{lm}(q, 0) \rangle. \tag{23}$$

Making again use of the plane wave expansion (13) and the orthogonality of the spherical harmonics, one derives the useful alternative expression

$$a_{lm}(q) = (-i)^l \overline{Y^*_{lm}(\Omega_q) \langle \exp(i\mathbf{q} \cdot \mathbf{u}) \rangle}. \tag{24}$$

Correspondingly to (19) the angular-averaged EISF can be expressed by a series of the form

$$\overline{\mathrm{EISF}(\mathbf{q})} = \sum_{l=0}^{\infty} \mathrm{EISF}_l(q), \tag{25}$$

with multipole coefficients

$$\mathrm{EISF}_l(q) = 4\pi \sum_{m=-l}^{l} |a_{lm}(q)|^2. \tag{26}$$

For $l = 0$, one obtains the isotropic component

$$\mathrm{EISF}_0(q) = |\langle j_0(qu) \rangle|^2 = \left| \overline{\langle \exp(i\mathbf{q} \cdot \mathbf{u}) \rangle} \right|^2. \tag{27}$$

We define $\delta^{(L)}_{\mathrm{aniso}}(q)$ to be the error of the Lth order multipole approximation to the angular-averaged EISF

$$\delta^{(L)}_{\mathrm{aniso}}(q) = \overline{\mathrm{EISF}(\mathbf{q})} - \sum_{l=0}^{L} \mathrm{EISF}_l(q), \tag{28}$$

and $\delta^{(0)}_{\mathrm{aniso}}(q)$ is thus the total anisotropy component, which may be expressed in the concise form

$$\delta^{(0)}_{\mathrm{aniso}}(q) = \overline{|\langle \exp(i\mathbf{q} \cdot \mathbf{u}) \rangle|^2} - |\overline{\langle \exp(i\mathbf{q} \cdot \mathbf{u}) \rangle}|^2. \tag{29}$$

If follows from the positivity of the multipole coefficients $\mathrm{EISF}_l(q)$ that

$$\delta^{(L)}_{\mathrm{aniso}}(q) \geq 0 \quad (L = 0, 1, 2, \ldots), \tag{30}$$

where the equal sign holds for perfectly isotropic motions.

C. Cumulant expansions

1. Intermediate scattering function

Writing the ISF in the form (11) shows that its Taylor expansion around $\mathbf{q} = \mathbf{0}$ gives access to the projected moments $\langle(\mathbf{n}\cdot\boldsymbol{\Delta}(t))^k\rangle$, where $\mathbf{n}$ is the unit vector in the direction of the momentum transfer vector $\mathbf{q}$. These moments and the corresponding cumulants, which are obtained from the corresponding Taylor series of $\log(F(\mathbf{q}, t))$, have been extensively discussed in the standard literature (see, for example, Refs. 5 and 22). Interesting in the context of this paper are the Taylor expansion for the angular-averaged ISF,

$$\overline{F(\mathbf{q},t)} = \sum_{k=0}^{\infty}\frac{(-1)^k q^{2k}}{(2k+1)!}\langle\Delta^{2k}(t)\rangle, \tag{31}$$

and the corresponding cumulant expansion

$$\overline{F(\mathbf{q},t)} = \exp\left(-\frac{q^2}{6}\langle\Delta^2(t)\rangle + \frac{q^4}{360}(3\langle\Delta^4(t)\rangle - 5\langle\Delta^2(t)\rangle^2) \mp \ldots\right). \tag{32}$$

For small times, such that $q^2\Delta^2(t) \ll 1$, the isotropic Gaussian approximation

$$\overline{F(\mathbf{q},t)} \approx \exp\left(-\frac{q^2}{6}\langle\Delta^2(t)\rangle\right) \tag{33}$$

is always valid and we note that expression (33) is exact for a few model systems, such as a freely diffusing particle in an isotropic medium and a particle diffusing in an isotropic harmonic potential.

2. EISF

To derive the cumulant expansion of the EISF, we use expression (23), noting that

$$\mathrm{EISF}_l(q) \overset{q\to 0}{\sim} q^{2l} \tag{34}$$

on account of the asymptotic form $j_l(z) \sim z^l/(2l+1)!!$ of the spherical Bessel functions for small arguments z.[19] Consequently, the Taylor expansion of $\mathrm{EISF}_l(q)$ contributes only terms of order $O \geq 2l$ in q to the corresponding Taylor expansion of the total angular-averaged EISF. Writing

$$\overline{\mathrm{EISF}(\mathbf{q})} = \sum_{k=0}^{\infty}(-1)^k q^{2k} M_{2k}, \tag{35}$$

the moments

$$M_{2k} = \lim_{t\to\infty}\frac{\langle\Delta^{2k}(t)\rangle}{(2k+1)!} \tag{36}$$

may thus be decomposed as

$$M_{2k} = \sum_{l=0}^{k} M_{2k}^{(l)}, \tag{37}$$

where $M_{2k}^{(l)}$ is the contribution of multipole order l. For the first few moments M_{2k}, one finds explicitly

$$M_0 = 1, \tag{38}$$

$$M_2 = \underbrace{\frac{1}{3}\langle u^2\rangle}_{M_2^{(0)}}, \tag{39}$$

$$M_4 = \underbrace{\frac{1}{36}\langle u^2\rangle^2 + \frac{\langle u^4\rangle}{60}}_{M_4^{(0)}} + \underbrace{\frac{4\pi}{225}\sum_{m=-2}^{2}|\langle u^2 Y_{2m}(\Omega_u)\rangle|^2}_{M_4^{(2)}}. \tag{40}$$

Here, it has been used that

$$u_m^{(l)} = \sqrt{\frac{4\pi}{2l+1}}u^l Y_{lm}(\Omega_u), \quad m = -l, \ldots, l, \tag{41}$$

are the components of the irreducible tensor products of order l, which are constructed from the components of $\mathbf{u}$ in the spherical coordinate representation[20]

$$u_{\pm 1}^{(1)} = \mp\frac{1}{\sqrt{2}}(u_x \pm i u_y), \quad u_0^{(1)} = u_z. \tag{42}$$

On account of $\langle u_{x,y,z}\rangle = 0$ we have therefore $\langle u_m^{(1)}\rangle = 0$ ($m = -1, 0, 1$), and using the latter property one obtains $M_2^{(1)} = M_4^{(1)} = 0$. With the above prerequisites the cumulant expansion for the angular-averaged EISF up to order q^4 is found to be

$$\overline{\mathrm{EISF}(\mathbf{q})} = \exp\left(-M_2 q^2 + \left\{M_4 - \frac{M_2^2}{2}\right\}q^4 + \ldots\right). \tag{43}$$

For $q^2\langle u^2\rangle \ll 1$, one can use the isotropic Gaussian approximation

$$\overline{\mathrm{EISF}(\mathbf{q})} \approx \exp\left(-\frac{q^2}{3}\langle u^2\rangle\right), \tag{44}$$

which follows also directly from expression (33), using that $\lim_{t\to\infty}\langle\Delta^2(t)\rangle = 2\langle u^2\rangle$ for confined motions in space.

III. EXAMPLES

A. Anisotropic motion in a harmonic potential

To illustrate the influence of anisotropic atomic motions on the EISF, we consider a simple model system, where the scattering atom moves in an anisotropic harmonic potential

$$V(\mathbf{u}) = \frac{K}{2}\left(u_x^2 + u_y^2 + \frac{1}{(1+\epsilon)^2}u_z^2\right) \tag{45}$$

with $K > 0$ and $\epsilon > -1$. Performing the ensemble average with the Gaussian Boltzmann factor $\exp(-V(\mathbf{u})/(k_B T))$ (k_B denotes the Boltzmann constant and T the absolute temperature) the corresponding MSPF is found to be

$$\langle u^2\rangle = \sigma^2(\epsilon(\epsilon+2)+3), \tag{46}$$

where

$$\sigma = \sqrt{\frac{k_B T}{K}}. \tag{47}$$

Introducing the amplitude $A(\mathbf{q}) = \langle\exp(i\mathbf{q}\cdot\mathbf{u})\rangle$, one obtains

$$A(\mathbf{q}) = \exp\left(-\frac{1}{2}\left(\sigma^2 q_x^2 + \sigma^2 q_y^2 + (1+\epsilon)^2\sigma^2 q_z^2\right)\right), \tag{48}$$

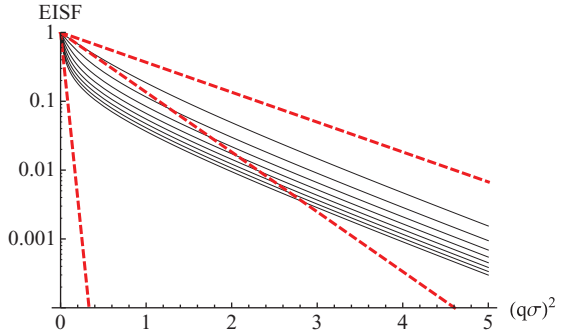

FIG. 1. The solid black lines display $\overline{\mathrm{EISF}(\mathbf{q})}$ corresponding to model (50) in a log-square plot, where $\epsilon = 1, 2, \ldots, 8$ (from top to bottom). The red dashed lines correspond to the isotropic Gaussian approximation (44) for $\epsilon = 0, 1, 8$, respectively.

such that

$$\mathrm{EISF}(\mathbf{q}) = |A(\mathbf{q})|^2 = \exp\left(-\left(\sigma^2 q_x^2 + \sigma^2 q_y^2 + (1+\epsilon)^2 \sigma^2 q_z^2\right)\right). \tag{49}$$

The isotropic angular average over the directions of $\mathbf{q}$ can be calculated analytically. Expressing $\mathbf{q}$ in spherical coordinates, $\mathbf{q} = q(\sin\theta\cos\phi, \sin\theta\sin\phi, \cos\theta)$, and performing an average over the total solid angle, one arrives at[23]

$$\overline{\mathrm{EISF}(\mathbf{q})} = \overline{|A(\mathbf{q})|^2} = \frac{\sqrt{\pi}\exp(-q^2\sigma^2)\mathrm{erf}(q\sigma\sqrt{\epsilon(\epsilon+2)})}{2q\sigma\sqrt{\epsilon(\epsilon+2)}}, \tag{50}$$

where erf(.) is the error function.[19] According to (27), the isotropic component $\mathrm{EISF}_0(q)$ is found by performing first the average of $A(\mathbf{q})$ over the directions of $\mathbf{q}$ and taking the square afterwards,[23]

$$\mathrm{EISF}_0(q) = |\overline{A(\mathbf{q})}|^2 = \frac{\pi\exp(-q^2\sigma^2)\mathrm{erf}(q\sigma\sqrt{\epsilon(\epsilon+2)/2})^2}{2q^2\sigma^2\epsilon(\epsilon+2)}. \tag{51}$$

In the limit $\epsilon \to 0$, where the potential $V(\mathbf{u})$ becomes isotropic, the isotropic Gaussian form (1) for the EISF is exact and the angular-averaged EISF coincides with its isotropic component,

$$\lim_{\epsilon\to 0}\overline{\mathrm{EISF}(\mathbf{q})} = \lim_{\epsilon\to 0}\mathrm{EISF}_0(q) = \exp\left(-q^2\sigma^2\right). \tag{52}$$

Figure 1 shows the model EISF (50) as a log-square plot, varying the anisotropy parameter according to $\epsilon = 1, 2, \ldots, 8$ from top to bottom (solid black lines). In addition, we show the isotropic Gaussian approximation (44) for $\epsilon = 0, 1, 8$, respectively (red dashed lines).

Concerning the anisotropy corrections of $\overline{\mathrm{EISF}(\mathbf{q})}$, it follows from the form of the potential $V(\mathbf{u})$ that $\mathrm{EISF}_1(q) = 0$ and that $\mathrm{EISF}_2(q) = 4\pi|a_{20}(q)|^2$. One finds explicitly[23]

$$\begin{aligned}\mathrm{EISF}_2(q) = {} & \frac{5\exp(-q^2\sigma^2((\epsilon+1)^2+1))}{16q^6\sigma^6\epsilon^3(\epsilon+2)^3} \\ & \times(\sqrt{2\pi}\exp(q^2\sigma^2(\epsilon+1)^2/2) \\ & \times(q^2\sigma^2\epsilon(\epsilon+2)-3)\mathrm{erf}(q\sigma\sqrt{\epsilon(\epsilon+2)}/\sqrt{2}) \\ & + 6q\sigma\sqrt{\epsilon(\epsilon+2)}\exp(q^2\sigma^2/2))^2. \end{aligned} \tag{53}$$

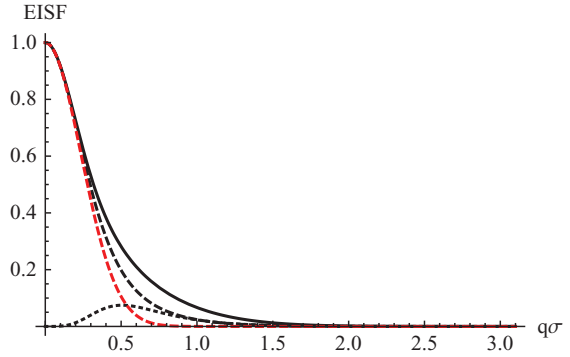

FIG. 2. Model EISF according to (50) for $\epsilon = 4$ (solid black line), the isotropic term $\mathrm{EISF}_0(q)$ (black dashed line), and the multipole term $\mathrm{EISF}_2(q)$ (black dotted line). The red dashed corresponds again to the Gaussian approximation.

Figure 2 shows the model EISF (50) for $\epsilon = 4$ together with the multipole terms $\mathrm{EISF}_0(q)$, $\mathrm{EISF}_2(q)$, and the isotropic Gaussian approximation. The value for ϵ is chosen to be compatible with the average anisotropy of atomic motions in the simulation study of lysozyme which will be presented in Sec. III B. Figure 3 displays the corresponding errors $\delta^{(L)}_{\mathrm{aniso}}(q)$ for $L = 0$ and $L = 2$ together with the error for the isotropic Gaussian approximation. The corresponding relative errors $\delta(q)/\overline{\mathrm{EISF}(\mathbf{q})}$ are displayed in Fig. 4. We note that the absolute error for the isotropic Gaussian approximation corresponds to the angular average of the anisotropy measure $S_{2,\mathrm{aniso}}(\mathbf{q})$ introduced in Ref. 11.

We finally give the first two terms of the cumulant expansion for the model EISF. Writing

$$\overline{\mathrm{EISF}(\mathbf{q})} = \exp\left(-c_2q^2 + c_4q^4 \mp \ldots\right), \tag{54}$$

one obtains from (50)

$$c_2 = \frac{1}{3}\sigma^2(\epsilon(\epsilon+2)+3), \tag{55}$$

$$c_4 = \frac{2}{45}\sigma^4\epsilon^2(\epsilon+2)^2. \tag{56}$$

These expressions are to be compared with the general form (43) for the cumulant expansion of the angular averaged EISF. The moments M_2 and M_4 can be computed

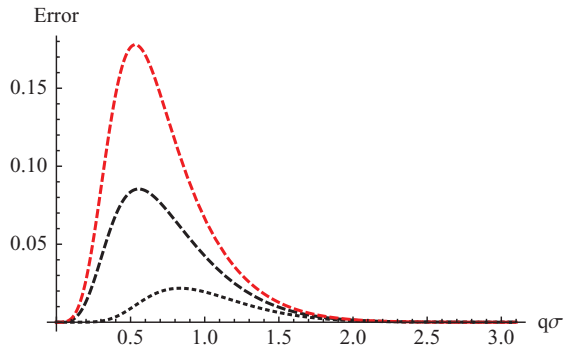

FIG. 3. The errors $\delta^{(0)}_{\mathrm{aniso}}(q)$ (black dashed line) and $\delta^{(2)}_{\mathrm{aniso}}(q)$ (black dotted line) corresponding to the multipole approximations of the model EISF shown in Fig. 2. The red dashed line represents the error of the Gaussian approximation.

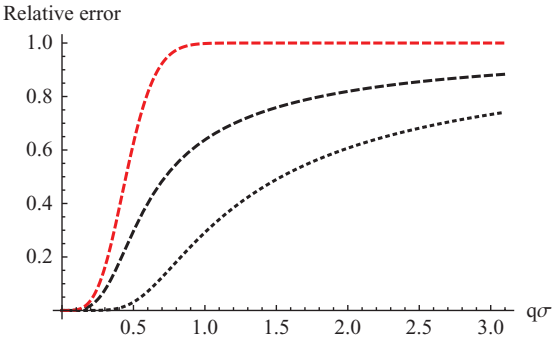

FIG. 4. Relative errors $\delta(q)/\overline{\mathrm{EISF}(\mathbf{q})}$ corresponding to the absolute errors shown in Fig. 3.

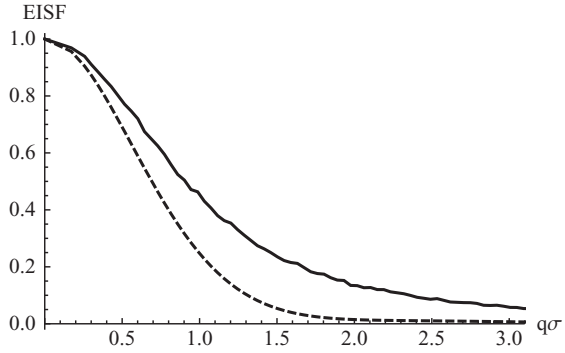

FIG. 5. Atom- and angular-averaged EISF for lysozyme computed from MD simulation (solid line) and the corresponding isotropic component (dashed line).

analytically by expressing the potential $V(\mathbf{u})$ in spherical coordinates $\{u, \theta, \phi\}$,

$$V(u,\theta) = \frac{Ku^2(2+\epsilon(\epsilon+2)(1-\cos(2\theta)))}{4(\epsilon+1)^2}, \tag{57}$$

and performing the ensemble averages $\langle \dots \rangle$ in these variables. Since the potential does not depend on ϕ the only multipolar contribution to M_4 is the term $(4\pi/225)|\langle u^2 Y_{2,0}(\Omega_u)\rangle|^2$. With these prerequisites one obtains[23]

$$M_2 = \frac{1}{3}\sigma^2(\epsilon(\epsilon+2)+3), \tag{58}$$

$$M_4 = \frac{1}{30}\sigma^4(\epsilon(\epsilon+2)(3\epsilon(\epsilon+2)+10)+15). \tag{59}$$

Inserting these results into $c_2 = M_2$ and $c_4 = M_4 - M_2^2/2$ (cf. Eq. (43)) the cumulants (55) and (56), respectively, are retrieved.

B. Molecular dynamics simulation study of lysozyme

To analyze the impact of anisotropic motions on the powder-averaged EISF of a realistic system, we performed a MD simulation of a lysozyme molecule in water. As starting structure, we used entry 1IO5 of the Protein Data Bank (PDB).[24] Adding the hydrogen atoms and 6805 water molecules as solvent lead to a total system size of 22 376 atoms. The simulations were performed with the Molecular Modeling Toolkit,[25] using the all-atom force field AMBER99[26] with periodic boundary conditions. Electrostatic interactions were treated with the method proposed by Wolf *et al.*,[27] using a cutoff radius of 1.4 nm. The integration time step was set to 1 fs and coordinates were saved every 50 fs for further analysis. After a preliminary minimization of the PDB structure the system was first equilibrated at constant temperature (300 K) and constant pressure (1 bar) using the Nosé-Andersen method.[28] The equilibrated system was then prolongated for a production run of 0.5 ns.

From the MD trajectory, we computed the exact angular-averaged EISF, performing a weighted sum over all 1961 protein atoms and applying weighting factors $\propto |b_{\alpha,\mathrm{inc}}|^2$. The calculation was performed with the program nMoldyn,[29] using a q-interval of $\Delta q = 0.25/\mathrm{nm}$ and averaging isotropically over up to 100 q-vectors per q-shell. The result is shown in Fig. 5 (solid line), together with the isotropic term $\mathrm{EISF}_0(q)$ (dashed line), which was computed as $\mathrm{EISF}_0(q) = |\langle j_0(qu)\rangle|^2$ (cf. Eq. (27)). To enable a comparison with the analytical example given before, the displayed functions are plotted on a dimensionless $q\sigma$-scale. Here,

$$\sigma = \sqrt{\langle u^2\rangle_a/3} = 0.172\,\mathrm{nm}, \tag{60}$$

where $\langle \dots \rangle_a$ is the average over the atoms of the lysozyme molecule. The deviation between the full angular-averaged EISF and the isotropic term being far from negligible, we analyzed this discrepancy in more detail by computing the motional anisotropies for the individual atoms from the respective displacement correlation matrix (the atomic index α is dropped),

$$\mathbf{C} = \begin{pmatrix} \langle u_x^2\rangle & \langle u_x u_y\rangle & \langle u_x u_z\rangle \\ \langle u_y u_x\rangle & \langle u_y^2\rangle & \langle u_y u_z\rangle \\ \langle u_z u_x\rangle & \langle u_z u_y\rangle & \langle u_z^2\rangle \end{pmatrix}. \tag{61}$$

Denoting the (positive) eigenvalues of $\mathbf{C}$ as λ_k ($k = 1, 2, 3$), we define the motional anisotropy through the dimensionless parameter

$$\epsilon = \sqrt{\frac{\lambda_{\max}}{\lambda_{\min}} - 1}. \tag{62}$$

If the atoms move in a harmonic potential of the form (45), expression (62) equals the parameter ϵ in this potential. Figure 6 displays a histogram of ϵ for the 1961 atoms in the lysozyme molecule. The ϵ-values range between $\epsilon_{\min} = 1.17$

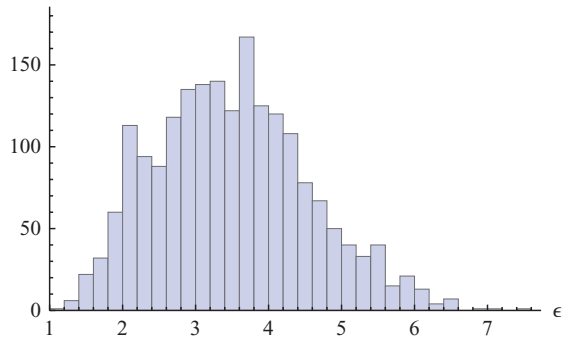

FIG. 6. Motional anisotropy for the atoms in lysozyme. The parameter ϵ is defined through Eq. (62).

and $\epsilon_{\max} = 7.54$, with a mean anisotropy of

$$\langle \epsilon \rangle_a \approx 3.5. \tag{63}$$

The motional anisotropy of the atoms in lysozyme is thus substantial.

IV. SUMMARY AND CONCLUSION

We have derived multipole and cumulant expansions for the ISF and the EISF of a single atom in a macroscopically isotropic sample which enable a systematic quantification of contributions from motional anisotropy. One could naïvely expect that performing powder averages of the scattering intensities removes all information on anisotropic displacements, but the result depends on the meaning of the term "displacement." Considering first the angular-averaged ISF for a single atom, we have shown that any information about motional anisotropy is, indeed, lost if the latter is described by the lag-time-dependent displacement $\mathbf{\Delta}(t)$. Information about the anisotropy in the displacement $\mathbf{u}(t)$ with respect to the respective static mean position is, in contrast, retained and the angular-averaged EISF is influenced by the static anisotropy of this dynamical variable. Due to the positivity of the multipole coefficients $\mathrm{EISF}_l(q)$ for a single atom, contributions from different atoms in a macromolecular system cannot average out, in contrast to what is stated in Ref. 11.

The impact of anisotropic atomic motions on a powder-averaged EISF have been illustrated by a simple analytical example and by a MD simulation study for lysozyme. The latter clearly demonstrates that anisotropic atomic motions contribute substantially to the EISF of a realistic system if the condition $q^2\langle u^2 \rangle \ll 1$ for the isotropic Gaussian approximation is not met. If the latter is used beyond the range of its validity, one obtains a more or less pronounced overestimation of the MSPF (see Fig. 1). Using the correlation matrices of the individual atomic position fluctuations we have shown that the motional anisotropy leads to a broad distribution for the ellipticity of the individual motions, with an average value of $\epsilon = 3.5$. Here, the effects of motional anisotropy, heterogeneity, and anharmonic effects are, or course, mixed, but the comparison to the "pure" case with comparable ellipticity, which is treated in the analytical example, confirms that the impact of motional anisotropy on the powder-averaged EISF is important.

The question which remains to be answered is how motional anisotropy can be accounted for in models for the EISF. In Ref. 13, it has been shown that good agreement between EISFs obtained from MD simulations and normal mode analysis can be obtained by using a model for motional heterogeneity in which the atoms in protein perform individually isotropic motions in a harmonic potential, such that the isotropic Gaussian approximation (1) for a single atom is correct. Comparing, however, the distribution of the MSPFs from the model and from simulation reveals that the motional heterogeneity is nevertheless not perfectly represented by the proposed model, as far as large MSPFs due to soft modes are considered. Here anisotropy plays, in fact, a more important role as for high frequency oscillations of stiff bonds. There seems thus to be some room for an improvement of the model, but one must be aware that neither simulation nor experimental data are precise enough to fit the corresponding additional parameters unambiguously.

ACKNOWLEDGMENTS

Guillaume Chevrot acknowledges financial support from the Agence Nationale de la Recherche, Contract No. ANR-2010-COSI-001-01.

[1] S. Lovesey, *Theory of Neutron Scattering from Condensed Matter* (Clarendon, Oxford, 1984), Vol. I.
[2] M. Bée, *Quasielastic Neutron Scattering: Principles and Applications in Solid State Chemistry, Biology and Materials Science* (Hilger, Bristol, 1988).
[3] J. Higgins and H. Benoît, *Polymers and Neutron Scattering* (Oxford University Press, New York, 1994).
[4] F. Gabel, D. Bicout, U. Lehnert, M. Tehei, M. Weik, and G. Zaccai, Q. Rev. Biophys. **35**, 327 (2002).
[5] J. Boon and S. Yip, *Molecular Hydrodynamics* (McGraw Hill, New York, 1980).
[6] H. Hartmann, F. Parak, W. Steigemann, G. Petsko, D. Ponzi, and H. Frauenfelder, Proc. Natl. Acad. Sci. U.S.A. **79**, 4967 (1982).
[7] K. H. Mayo, D. Kucheida, F. Parak, and J. C. Chien, Proc. Natl. Acad. Sci. U.S.A. **80**, 5294 (1983).
[8] W. Doster, S. Cusack, and W. Petry, Nature (London) **337**, 754 (1989).
[9] G. Zaccai, Science **288**, 1604 (2000).
[10] T. Ichiye and M. Karplus, Proteins **2**, 236 (1987).
[11] A. Tokuhisa, Y. Joti, H. Nakagawa, A. Kitao, and M. Kataoka, Phys. Rev. E **75**, 041912 (2007).
[12] L. Meinhold, D. Clement, M. Tehei, R. Daniel, J. Finney, and J. Smith, Biophys. J. **94**, 4812 (2008).
[13] G. R. Kneller and K. Hinsen, J. Chem. Phys. **131**, 045104 (2009).
[14] Z. Yi, Y. Miao, J. Baudry, N. Jain, and J. C. Smith, J. Phys. Chem. B **116**, 5028 (2012).
[15] C. J. Burden and A. J. Oakley, Phys. Biol. **4**, 79 (2007).
[16] K. Hinsen, Bioinformatics **24**, 521 (2008).
[17] C. C. Wilson, Crystallogr. Rev. **15**, 3 (2009).
[18] G. R. Kneller, Mol. Phys. **83**, 63 (1994).
[19] *NIST Handbook of Mathematical Functions*, edited by F. W. J. Olver, D. W. Lozier, R. F. Boisvert, and C. W. Clark (Cambridge University Press, 2010).
[20] M. Rose, Proc. Phys. Soc., London, Sect. A **67**, 239 (1954).
[21] A. Edmonds, *Angular Momentum in Quantum Mechanics* (Princeton University Press, Princeton, NJ, 1957).
[22] A. Rahman, K. Singwi, and A. Sjölander, Phys. Rev. **126**, 986 (1962).
[23] MATHEMATICA 8.0 (Wolfram Research, Inc., Champaign, IL, 2011).
[24] N. Niimura, Y. Minezaki, T. Nonaka, J. C. Castagna, F. Cipriani, P. Høghøj, M. S. Lehmann, and C. Wilkinson, Nat. Struct. Biol. **4**, 909 (1997).
[25] K. Hinsen, J. Comput. Chem. **21**, 79 (2000).
[26] J. Wang, P. Cieplak, and P. Kollman, J. Comput. Chem. **21**, 1049 (2000).
[27] D. Wolf, P. Keblinski, S. R. Phillpot, and J. Eggebrecht, J. Chem. Phys. **110**, 8254 (1999).
[28] S. Nosé, J. Chem. Phys. **81**(1), 511 (1984).
[29] T. Rog, K. Murzyn, K. Hinsen, and G. R. Kneller, J. Comput. Chem. **24**, 657 (2003).